Adhesion-Associated and PKC-Modulated Changes in Serine/Threonine Phosphorylation of p120-Catenin†

Xiaobo Xia, Debbie J. Mariner, and Albert B. Reynolds*

Department of Cancer Biology, Vanderbilt University, PRBII 771, Nashville, Tennessee 37232-6840

Received April 14, 2003; Revised Manuscript Received May 30, 2003

ABSTRACT: p120-catenin (p120) was originally identified as a tyrosine kinase substrate, and subsequently shown to regulate cadherin-mediated cell−cell adhesion. Binding of the p120 Arm domain to E-cadherin appears to be necessary to maintain adequate cadherin levels for strong adhesion. In contrast, the sequence amino-terminal to the Arm domain confers a negative regulatory function that is likely to be modulated by phosphorylaton. Several agents that induce rapid changes in cell−cell adhesion, including PDBu, histamine, thrombin, and LPA, result in significant changes in p120 S/T phosphorylation. In some cases, these changes are PKC-dependent, but the relationship among adhesion, PKC activation, and p120 phosphorylation is unclear, in part because the relevant p120 phosphorylation sites are unknown. As a crucial step toward directly identifying the function of these modifications in adhesion, we have used two-dimensional tryptic mapping and site-directed mutagenesis to pinpoint the constitutive and PKC-modulated sites of p120 S/T phosphorylation. Of eight sites that have been identified, two were selectively phosphorylated *in vitro* by GSK3β, but *in vivo* treatment of cells with GSK3β inhibitors did not eliminate these sites. PKC stimulation *in vivo* induced potent dephosphorylation at S268, and partial dephosphorylation of several additional sites. Surprisingly, PKC also strongly induced phosphorylation at S873. These data directly link PKC activation to specific changes in p120 phosphorylation, and identify the target sites associated with the mechanism of PKC-dependent adhesive changes induced by agents such as histamine and PDBu.

p120 catenin (hereafter p120) was originally identified as a Src and receptor tyrosine kinase substrate (*1*, *2*), and subsequently revealed as a prominent binding partner of classical cadherins (*3*−*5*). Cadherins comprise a major class of transmembrane cell−cell adhesion molecules with roles in development, morphogenesis, and cancer (reviewed in ref *6*). At the molecular level, cadherin extracellular domains bind to one another to generate adherens junctions between neighboring cells. The cytoplasmic domains interact with the armadillo repeat domain proteins β-catenin, plakoglobin, and p120. β-Catenin (or plakoglobin) binds further with α-catenin, which physically links the complex to the actin cytoskeleton (*7*−*10*). In contrast, p120 does not bind α-catenin, and is postulated to indirectly regulate the cytoskeletal linkage, possibly through modulation of Rho GTPases (*11*−*15*).

An extensive literature implies that p120 can both positively and negatively regulate cell adhesiveness (*16*−*19*), which likely depends on signaling inputs that regulate its activity. Using a p120-deficient SW48 colon carcinoma cell line, we showed previously that restoring p120 expression substantially increases E-cadherin levels and rescues epithelial morphology by unidentified mechanisms that are dependent on the direct interaction between these proteins (*20*). The rescue was much more efficient using constructs lacking the amino-terminal domain. This activity is likely responsible for the positive effects of p120, and necessary to maintain E-cadherin abundance at levels sufficient to mediate strong cell−cell adhesion (*20*). In contrast, constructs including the amino-terminal domain dampened this otherwise positive effect, reflecting the presence of negative regulatory sequences. Our data are consistent with results in Colo205 cells, in which cadherin adhesiveness was restored by p120 isoforms lacking the amino terminus, but not by isoforms that retained these sequences (*16*). The amino-terminal domain contains all of the previously identified tyrosine phosphorylation sites (*21*), but serine and threonine phosphorylation sites have not been mapped. A working model suggests that signaling molecules that modulate cadherin cell−cell adhesion act in part by inducing changes in p120 tyrosine (Y)[1] and/or serine/threonine (S/T) phosphorylation, and thereby negatively modulate the otherwise positive action of p120 on E-cadherin adhesiveness.

Recent studies implicate S/T phosphorylation in this process (*16*, *17*, *22*, *23*). Under normal conditions of cell

† This work was supported in part by National Institutes of Health Grant CA55724, and by the Vanderbilt-Ingram Cancer Center through Cancer Center Support Grant CA68684-06.

* To whom correspondence should be addressed: Department of Cancer Biology, Vanderbilt University, PRBII 771, Nashville, TN 37232-6840. Phone: (615) 343-9532. Fax: (615) 936-6399. E-mail: al.reynolds@vanderbilt.edu.

[1] Abbreviations: Arm, armadillo; PKC, protein kinase C; LPA, lysophosphatidic acid; VEGF, vascular endothelial growth factor; S, serine; Y, tyrosine; T, threonine; PDBu, phorbol 12,13-dibutyrate; BisI, bisindolylmaleimide; PAA, phosphoamino acid analysis; TLC, thin-layer chromatography.

10.1021/bi034597h CCC: $25.00
Published on Web 07/11/2003

culture, p120 is constitutively phosphorylated on serine and threonine (*2*, *24*). In many epithelial and endothelial cell lines, pharmacologic activation of protein kinase C (PKC) induces significant S/T dephosphorylation of p120 (*22*, *23*), as evidenced by discreet p120 bandshifts on SDS−polyacrylamide gels, and by direct measurements of p120 S/T phosphorylation levels. p120 dephosphorylation is also induced by physiologically relevant agents such as histamine, thrombin, lysophosphatidic acid (LPA) (*23*), and vascular endothelial growth factor (VEGF) (*25*). These agents dramatically reduce adhesiveness in some cell types, often in a PKC-dependent manner (*22*, *23*, *26*−*28*). Defects in Colo205 cell−cell adhesion have also been correlated with changes in p120 S/T phosphorylation. These effects can be partially reversed by staurosporine, a broad spectrum kinase inhibitor which also induces changes in p120 S/T phosphorylation. While these observations strongly support a role for p120 S/T phosphorylation in dynamically modulating cadherin function, direct mechanistic evidence is lacking, in part because the relevant sites have not been identified.

To directly address the role of p120 S/T phosphorylation in cadherin function, and to link p120 modification to specific signaling pathways, we aim to generate p120 S/T mutants that can selectively reveal specific roles for individual phosphorylation sites. Here, as a crucial step toward advancing these goals, we employed two-dimensional tryptic mapping methods to identify all major p120 sites of constitutive and PKC-induced S/T phosphorylation. Eight sites were identified, five of which mapped to the amino-terminal phosphorylation domain, a stretch of approximately 100 amino acids shown previously to contain the major tyrosine phosphorylation sites induced by Src (*21*). The major site dephosphorylated by PKC activation was S268, although partial dephosphorylation was detected at several sites. Surprisingly, the most striking effect of PKC activation was a strong induction of phosphorylation at S873, an event not predicted by previous evidence. Thus, several pathways act through PKC to post-translationally modify p120 at multiple sites. We conclude that pathways affecting cadherin function through PKC act both directly and indirectly on p120 and are likely to regulate adhesion through this mechanism.

EXPERIMENTAL PROCEDURES

Antibodies and Other Reagents. Anti-p120 mAbs pp120 (Transduction Laboratories), 8D11 (*29*), and 15D2 (*29*) (Zymed) have been characterized extensively (*29*). Monoclonal antibody 12CA5 (Boehringer Mannheim Corp.) recognizes the hemagglutinin (HA) epitope tag. pCMX-GSK3β-HA, which expresses HA-tagged GSK3β, was provided by R. Wisdom (Vanderbilt University). pCMX-GSK3β K85M/86I-HA, which encodes a kinase-inactivated form of GSK3β, was constructed by site-directed mutagenesis as described below.

The following protein kinase inhibitors or activators were used: staurosporine, bisindolylmaleimide I (BisI), and phorbol 12,13-dibutyrate (PDBu) from Sigma.

Mutagenesis. The murine p120 deletion mutants used in this study have been described previously (*30*). Point mutations were generated by site-directed mutagenesis using QuickChange mutagenesis (Stratagene) according to the manufacturer's instructions, except that Turbo *pfu* polymerase (Stratagene) was used for all amplification reactions. All S/T point mutations of p120 were constructed initially in RcCMV mp120-1A and verified by DNA sequencing.

Cell Culture and Transient Transfection. NIH3T3 (murine fibroblast), HCT116 (human colorectal carcinoma), and Colo205 (human colorectal carcinoma) cells were obtained from American Type Culture Collection and cultured in Dulbecco's modified Eagle's medium (DMEM, Hyclone). LNCaP cells (human prostate carcinoma), generously provided by S. Brady-Kalnay, were cultured in RPMI 1640 (Life Technologies, Inc.). All media were supplemented with 10% heat-inactivated fetal bovine serum (Hyclone) and 1% penicillin-streptomycin (Life Technologies, Inc.). For cell treatments, reagents dissolved in DMSO were added to medium directly with a 1:1000 dilution. The same amount of DMSO was used as a control.

Transient transfections were performed with SuperFect transfection reagent (Qiagen) according to the manufacturer's directions; 5 μg of total DNA and 25 μL of SuperFect were used for each transfection per 60 mm dish. For cotransfection experiments, equal amounts of each plasmid were transfected. *In vivo* labeling or cell lysate preparation was performed 24 h after transfection.

Mouse p120 constructs used in transient transfections include RcCMV, RcCMV, mp120-1A (wild type or S/T to alanine point mutants), RcCMV mp120-3A, RcCMV mp120-4A, RcCMV mp120-1NΔ29-233, and RcCMV mp120-1NΔ234-387.

In Vivo Labeling of p120. Cells were 80−90% confluent on the day of *in vivo* labeling. Cells were washed twice with Tris-buffered saline (pH7.4) and starved for 15 min in phosphate-free DMEM (Life Technologies, Inc., 4 mL/100 mm dish, 1.5 mL/60 mm dish) containing 4% dialyzed fetal bovine serum (Life Technologies, Inc.). ^{32}P-labeled H_3PO_4 (0.5 mCi/μL in H_2O, carrier-free, ICN Biomedicals Inc.) was then added directly to the medium (1 mCi/100 mm dish, 0.35 mCi/60 mm dish), and cells were incubated in this medium for 4 h. Cell lysate preparation and immunoprecipitation were then performed as described below.

Cell Lysate Preparation and Immunoprecipitation. For phosphopeptide mapping, metabolically labeled cells were washed once with Tris-buffered saline (TBS, pH 7.4) and lysed with 1 mL per dish of ice-cold RIPA buffer [50 mM Tris (pH 7.4), 150 mM NaCl, 1% Nonidet P-40, 0.5% deoxycholic acid, and 0.1% SDS] containing protease and phosphatase inhibitors (1 mM phenylmethanesulfonyl fluoride, 5 μg/mL leupeptin, 2 μg/mL aprotinin, 1 mM EDTA, and 50 mM NaF) for 5 min. Lysates were precleared by centrifugation at 14 000 rpm for 10 min. Then 4 μg of primary monoclonal antibodies (mAb) was added to the supernatants, and incubated for 1 h at 4 °C with end-over-end rotation. mAb pp120 or 15D2 was used for endogenous p120, while mAb 8D11, which does not react with human p120, was used to selectively immunoprecipitate transfected murine p120. Then 20 μL of a protein A−Sepharose 4B bead slurry (Amersham Pharmacia Biotech; 1:1 slurry of beads and phosphate-buffered saline at pH 7.4) coupled to a rabbit anti-mouse IgG bridge antibody (Jackson Immunoresearch, Inc.) was added to lysates and the mixture incubated at 4 °C for an additional 1 h. Immunoprecipitates were washed four times with RIPA lysis buffer, resuspended in 2× Laemmli sample buffer, and boiled at 100 °C for 5 min. Protein samples were separated by SDS−polyacrylamide gel

electrophoresis (SDS−PAGE) and transferred to polyvinylidene difluoride (PVDF) membranes (Millipore) for phosphopeptide tryptic mapping.

In Vitro Kinase Assay. HCT116 cells were cotransfected with 2.5 μg of RcCMV mp120-1A (wild type or S/T to alanine point mutants) and 2.5 μg of pCMX GSK3β-HA (wild type or K85M/K86I mutant). Cell lysis and immunoprecipitation procedures were performed as described above, except that 3 μg of both p120 antibody (8D11) and HA tag antibody (12CA5) were added to lysates to immunoprecipitate both p120 and GSK3β together. Immunoprecipitates were washed four times with ice-cold RIPA buffer and twice with Tris-buffered saline (pH 7.4). Then immunoprecipitates were incubated with 20 μL of serine/threonine kinase buffer [20 mM HEPES (pH 7.4) and 10 mM $MgCl_2$] containing 10 μCi of [γ-^{32}P]ATP (ICN Biomedicals Inc.) for 30 min at room temperature with constant agitation. Reactions were terminated by washing the mixture twice with RIPA buffer containing 5 mM EDTA followed by boiling in 2× Laemmli sample buffer for 5 min.

Phosphopeptide Tryptic Mapping and Phosphoamino Acid Analysis. Phosphoproteins labeled *in vivo* or *in vitro* were separated by SDS−PAGE and transferred to PVDF membranes. After visualization by autoradiography, expected phosphoprotein bands were cut out and phosphoproteins were cleaved from the membrane with 10 μg/mL L-(tosylamino-2-phenyl)ethyl chloromethyl ketone-treated bovine pancreas trypsin (TPCK-trypsin, Worthington) as described previously (*21*). The resulting peptides were then subjected to two-dimensional phosphopeptide mapping or phosphoamino acid analysis using thin-layer cellulose plates (VWR) according to the procedures described in detail previously (*31*). Briefly, for two-dimensional phosphopeptide mapping, digested phosphopeptides were separated in the first dimension by electrophoresis using a Hunter thin-layer electrophoresis chamber with pH 1.9 buffer (1.0 kV, 30 min) and then in the second dimension by ascending chromatography with phosphochromatography buffer. For phosphoamino acid analysis (PAA), digested total phosphopeptides or individual phosphopeptides recovered from TLC mapping plates were acid-hydrolyzed at 110 °C in 6 N HCl for 1 h. Samples were then lyophilized and analyzed by first-dimension (pH 1.9 buffer, 1.5 kV, 20 min) and second-dimension (pH 3.5 buffer, 1.3 kV, 16 min) electrophoresis. To identify the phosphoamino acids, samples were mixed with phosphoserine, phosphothreonine, and phosphotyrosine standards before they were loaded onto TLC plates. After two-dimensional electrophoresis, standards were visualized with ninhydrin. Finally, TLC plates for both tryptic mapping and PAA were visualized by radiography with KODAK X-OMAT AR X-ray films exposed with an intensifying screen at −70 °C.

Generation of Colo205 Stable Cell Lines Using the Retroviral Expression System. Construction of the pMS shuttle vector and LZRS retroviral vector pLZRS-MS-IRES-neo has been described previously (*20*). cDNAs for mp120-3A or mp120-4A (and mutants derived from these cDNAs) were first subcloned into pMS, and then moved into pLZRS-MS-IRES-neo vectors using the unique restriction sites of *Sgf*I and *Sfi*I. Calcium phosphate transfection of the viral packaging Phoenix 293 cells, viral harvest, and infection of Colo205 cells were performed as described previously (Nolan lab website at http://www.stanford.edu/group/nolan; also see ref *20*). Colo205 stable cell lines were established by G418 selection.

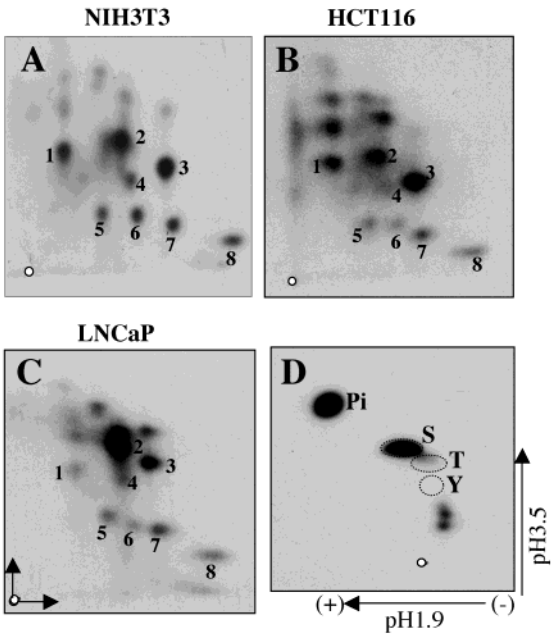

FIGURE 1: Major serine/threonine phosphorylation sites of p120 are conserved among different cell lines and species. (A−C) Two-dimensional tryptic phosphopeptide maps of endogenous p120 from the indicated murine (A) and human (B and C) cell lines. Prominent peptides (spots) that are observed reproducibly in all of the cell lines that were tested are numbered from 1 to 8. Samples were loaded at the origin (o), and arrows that originate from loading origins indicate the direction of electrophoresis (horizontal, toward the cathode) and chromatography (vertical), respectively. (D) Phosphoamino acid analysis (PAA) of *in vivo*-labeled endogenous p120 from HCT116 cells showed that most phosphorylation was on serine, but trace amounts were also detected on threonine. Positions of phosphoserine (S), phosphothreonine (T), and phosphotyrosine (Y) standards are circled. The sample loading origin is indicated (o), and arrows indicate the directions of electrophoretic migration toward the anode in the first (pH 1.9) and second (pH 3.5) dimensions. See Figure 3J for a schematic illustration of the PAA map.

RESULTS

S/T Phosphorylation Sites Are Conserved across Cell Lines and Species. To characterize the p120 S/T phosphorylation status *in vivo*, two-dimensional tryptic phosphopeptide mapping was performed on endogenous p120 from different human and murine cell lines. These maps displayed very similar patterns of approximately 14−18 phosphopeptides (Figure 1A−C), although the density of individual phosphopeptides varied between cell lines and from experiment to experiment. Phosphoamino acid analysis (PAA) of p120 from HCT116 cells showed that most of the phosphorylation (>90%) occurred on serine, although threonine phosphorylation was also detected (Figure 1D). No phosphotyrosine was detected. Thus, consistent with previous reports (*21*, *32*), under normal circumstances, p120 is almost exclusively phosphorylated on S/T. Phosphopeptides 1−8 were chosen for identification because they were prominently phosphorylated and observed consistently in most of the cell lines that were tested.

Identification of Major p120 S/T Phosphorylation Sites. p120 contains 71 serine and 47 threonine residues. To narrow the search to a manageable number of candidate sites, pilot

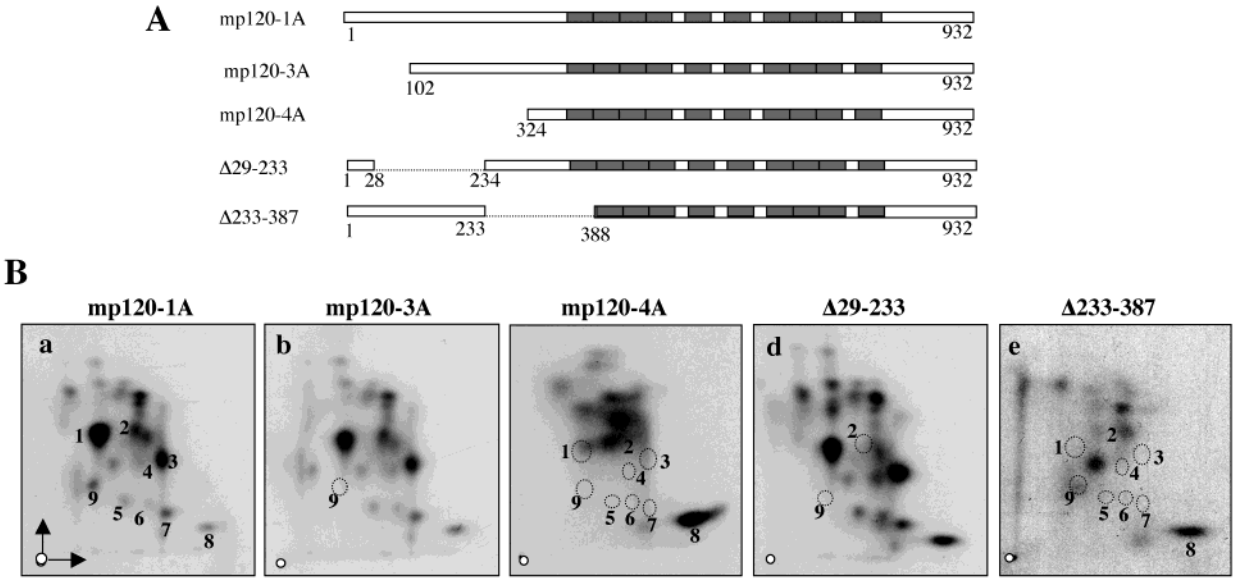

FIGURE 2: Initial localization of the major S/T sites by isoform and deletion analysis. (A) Schematic illustration of murine p120 isoforms and deletion constructs used in this study. Deleted regions are illustrated with dotted lines. (B) Two-dimensional tryptic maps of different mp120 isoforms and deletion mutants. The indicated p120 constructs were transiently overexpressed and proteins metabolically labeled with [^{32}P]orthophosphate in HCT116 cells. The transfected murine p120 was selectively recovered from the human HCT116 cell line by immunoprecipitation with mAb 8D11 and then analyzed by two-dimensional tryptic mapping. Peptides absent from each map are highlighted with dashed circles around their predicted location.

studies were carried out using a panel of murine p120 isoforms and deletion mutants (Figure 2A). The strategy involved transiently transfecting murine p120 into human (HCT116) cells, and then selectively recovering the transfected p120 (after *in vivo* labeling) by immunoprecipitation with mAb 8D11, which recognizes murine but not human p120. This approach allows us to recover the transfected murine p120 from human cells without interference from the endogenous p120. The tryptic map of murine p120-3A (Figure 2B, panel b) was very similar to the map derived from the endogenous human p120 isolated from the same cells (Figure 1B). Thus, the phosphorylation sites are conserved between murine and human p120, and transfected murine p120 is accurately phosphorylated in human cells.

As shown in Figure 2B, the transfected wild-type mp120-1A isoform contained the same major spots as mp120-3A with the exception of spot 9, which was absent from mp120-3A. This peptide was also absent from p120 containing a deletion of residues 29−233 (Figure 2B, panel d). Together, these data suggested that peptide 9 was located in an amino-terminal region between amino acids 29 and 102. With the exception of spots 2 and 8, all the major spots were eliminated in mp120-4A (Figure 2B, panel c). Thus, spots 1 and 3−7 were tentatively assigned to the region between amino acids 102 and 324. Peptide 8 was detected in deletion Δ233−387 (Figure 2B, panel e), suggesting that its location was carboxy-terminal to residue 387. Peptide 2 is located C-terminal to amino acid 324 because it was present in mp120-4A. However, for reasons that are unclear, peptide 2 was lost from the deletion mutant Δ29−233 (Figure 2B, panel d). It is possible that the deletion of amino acids 29−233 causes conformational changes that eliminate the phosphorylation at this site. These data demonstrate that most of the major sites are concentrated in an amino-terminal region that has been previously termed the phosphorylation domain based on assignment of the majority of the Src-induced tyrosine phosphorylation sites (*21*).

To discriminate between serine and threonine phosphorylation, each spot was individually recovered from TLC plates and subjected to phosphoamino acid analysis (Figure 3). Results showed that spots 1−4, 6, and 9 contained only phosphoserine, whereas spots 7 and 8 contained only phosphothreonine. Spot 5 contained both phosphoserine and phosphothreonine.

On the basis of the preliminary mapping information, and clues from the two-dimensional migration characteristics of the spots, we chose candidate sites for reanalyzis after mutation to alanine. As shown in Figure 4, alanine substitutions for S288 (S288A), S268 (S268A), T910 (T910A), and S122 (S122A) resulted in the elimination of phosphopeptide spots 1, 3, 8, and 9, respectively (panels E, D, I, and B of Figure 4, respectively). The phosphorylation site of peptide 9 (S122) was not in accordance with our previous prediction of a location between amino acids 29 and 102. Apparently, residues 1−112, present in p120-1A, but not in p120-3A, are necessary for phosphorylation at residue S122. The S252A mutation eliminated two spots, spots 4 and 6 (Figure 4C). Likewise, the T310A mutation removed both spots 5 and 7 (Figure 4F). These putative two-spot peptides were further analyzed by partial acid hydrolysis of each spot, and resulting peptide "fingerprints" were compared. As implied by the above data, the patterns for spots 4 and 6 were identical, as were the patterns from spots 5 and 7 (compare panels D and F of Figure 3, and panels E and G of Figure 3). Thus, spots 4 and 6 are partial tryptic products of peptides containing S252, and spots 5 and 7 are partial tryptic products of peptides containing T310. This result was further confirmed by tryptic maps from GSK3β *in vitro* kinase assays (described later in Figure 5).

Since peptide 5 contains both phosphoserine and phosphothreonine, and S312 is the only serine located in the tryptic peptide containing T310, it is likely that S312 is also phosphorylated *in vivo*. Indeed, the S312A mutation eliminated spot 5 from the map completely (Figure 4H), but spot

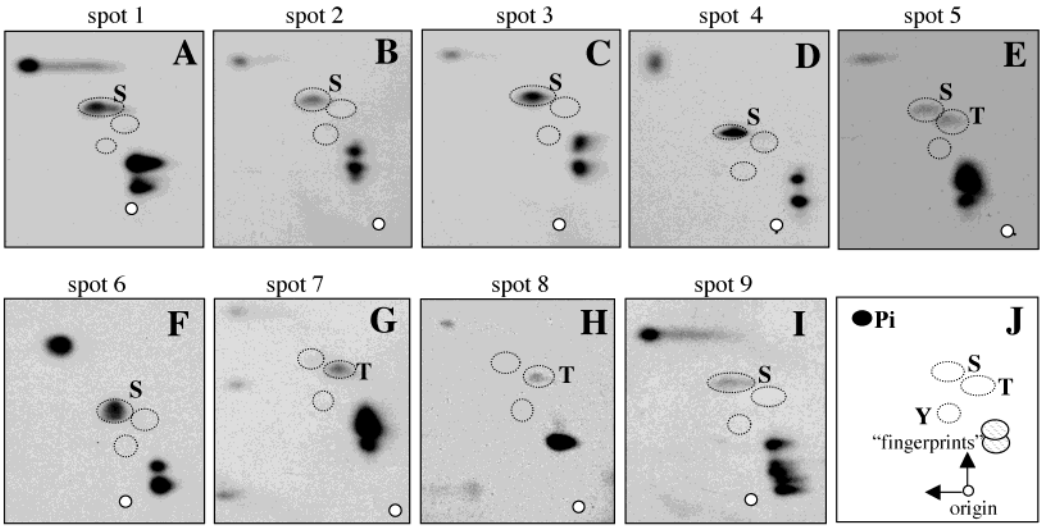

FIGURE 3: Phosphoamino acid analysis (PAA) of individual p120 phosphopeptides. (A−I) Following two-dimensional tryptic mapping, individual phosphopeptides were recovered from TLC plates and subjected to two-dimensional mapping for PAA. Positions of phosphoamino acid standards are illustrated with circles. (J) Schematic showing locations of phosphoserine (S), phosphothreonine (T), phosphotyrosine (Y), and free orthophosphate (P_i). The striped spots labeled with "fingerprints" refer to the partial hydrolysis products, which are unique to each peptide.

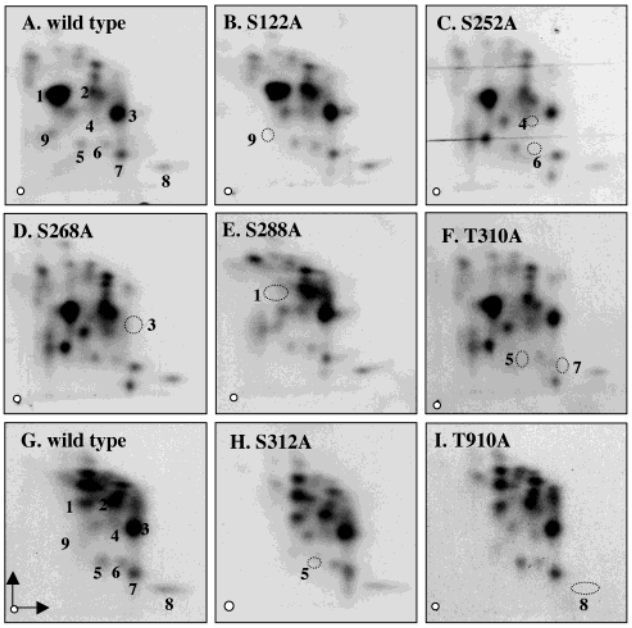

FIGURE 4: Direct identification of major *in vivo* phosphorylation sites by mutational analysis. Each candidate S/T phosphorylation site was mutated to alanine. The constructs were expressed and proteins labeled *in vivo* in HCT116 cells and analyzed by two-dimensional tryptic mapping. Alanine mutations at S122, S252, S268, S288, T310, S312, and T910 eliminated specific phosphopeptide spots as indicated in panels A−I (predicted locations are circled). Because of experimental variation from one batch of maps to the next, wild-type p120 control maps are shown for each experimental run. Panel A is the control for panels B−F. Panel G is the control for panels H and I.

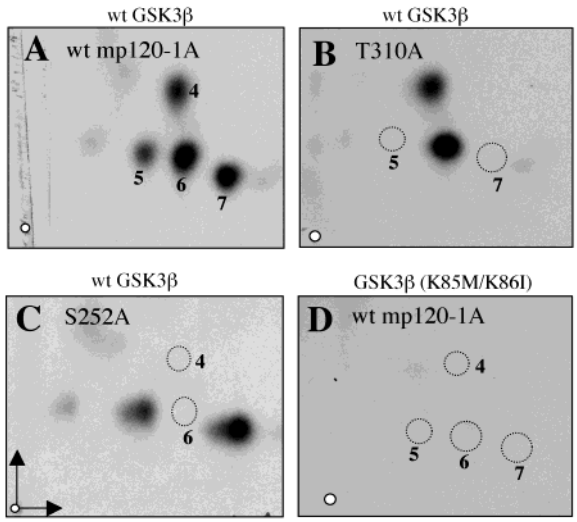

FIGURE 5: GSK3β selectively phosphorylates p120 on S252 and T310 *in vitro*. Wild type (A−C) or kinase dead GSK3β-HA (D) was transiently co-overexpressed in HCT116 cells with either wild-type mp120-1A (A and D) or mp120-1A mutants containing alanine substitutions at either T310 (B) or S252 (C). The overexpressed GSK3β-HA and p120 proteins were immunoprecipitated together with p120 mAb 8D11 and HA-tag mAb 12CA5, and *in vitro* kinase assays were performed as described in Experimental Procedures. *In vitro*-labeled p120 was then subjected to phosphopeptide tryptic mapping. The resulting maps show selective phosphorylation of p120 by GSK3β on four spots corresponding to spots 4−7 on maps from *in vivo*-labeled p120. As in the case of *in vivo*-labeled p120, *in vitro* spots 4 and 6 were eliminated by the S252A mutation, and spots 5 and 7 were eliminated by the T310A mutation.

7 was unaffected. Since the T310A mutation eliminated both spots, one possibility is that spot 5 represents a peptide phosphorylated on both T310 and S312, whereas spot 7 is phosphorylated on T310 alone. If phosphorylation of T310 is a prerequisite for phosphorylation of S312, then eliminating T310 could result in loss of phosphorylation at both T310 and S312.

The results of the mapping data are summarized in Table 1. The only major site that we were not able to identify is spot 2.

GSK3β Can Phosphorylate p120 in Vitro. p120 contains several consensus phosphorylation sites (SXXXpS) for the S/T kinase GSK3β, a kinase known to regulate the stability of β-catenin (*33*−*35*). To evaluate whether GSK3β regulates p120, we initially asked whether GSK3β could phosphorylate

Table 1: Summary of Major p120 S/T Phosphorylation Sites *in Vivo*[a]

Peptide	Phosphorylated residue(s)	Tryptic fragment	Characteristics
9	S122	^{102}MQEPGQIVETYTEEDPEGAMS^{122}VVSVETTDDGTTR/R $^{135/6}$	Only in mp120-1A
4, 6	S252	^{250}APS^{252}R ^{253}	GSK3β *in vitro* site
3	S268	^{265}VGGS^{268}SVDLHR ^{274}	PKC-dephosphorylated
1	S288	^{288}S^{288}MGYDDLDYGMMSDYGTAR/R $^{306/307}$	
7	T310	^{308}TGT^{310}PSDPR/R/R $^{315/316/317}$	GSK3β *in vitro* site
5	T310, S312	^{308}TGT^{310}PS^{312}DPR/R/R $^{315/316/317}$	
10	S873	^{873}S^{873}DK/K/PDR/EEIPMSNMGSNTK/SLDNNYSTLNER ^{904}	PKC-phosphorylated
8	T910	^{910}T^{910}LDR ^{913}	Absent in Colo205 cells
2	unknown		Present in isoform 4A

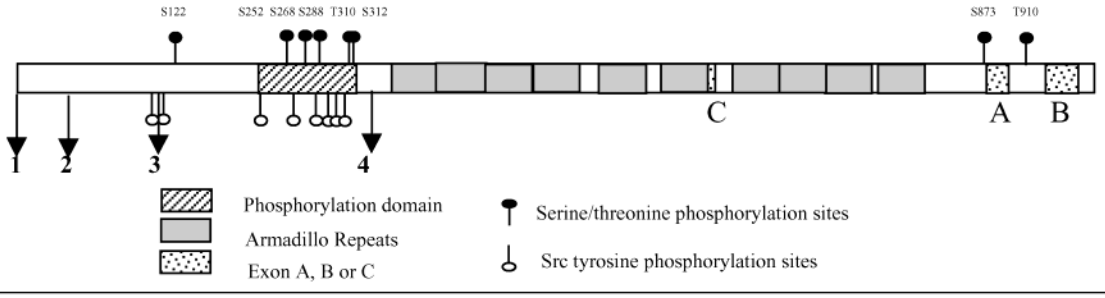

[a] Trypsin cleaves after lysine (K) or arginine (R) but cuts inefficiently between the adjacent R or K. It also does not cut efficiently when R and K is followed by glutamic acid (E) or aspartic acid (D). It does not cut when a proline (P) directly follows an R or K. Amino acid numbers are based on the murine p120 isoform 1A sequence.

p120 *in vitro*. HA-tagged GSK3β and wild-type mp120-1A were cotransfected into HCT 116 cells and then immunoprecipitated together using p120 mAb 8D11 and HA-tag mAb 12CA5. p120 was then phosphorylated with the GSK3β *in vitro* kinase assay and analyzed by tryptic mapping. The *in vitro*-labeled p120 revealed four spots corresponding to spots 4−7 on the *in vivo* maps (compare Figure 5A to Figure 1B). Although S252 and T310 do not match known GSK3β consensus motifs, it appears that GSK3β efficiently phosphorylates these sites *in vitro* since the S252A mutation eliminated spots 4 and 6 whereas the T310A mutation eliminated spots 5 and 7 (panels B and C of Figure 5, respectively). As expected, kinase dead GSK3β did not phosphorylate p120 on any of the sites (Figure 5D). Thus, S252 and T310 are efficiently and selectively phosphorylated *in vitro* by GSK3β. The four spots associated with these residues comigrate exactly with p120 spots 4−7 identified *in vivo*. However, we could not obtain evidence that these sites are phosphorylated by GSKβ *in vivo*. When we treated HCT116 cells with either lithium chloride (20 mM) or GSK inhibitor I (Calbiochem), we did not see any change in phosphorylation of these sites (data not shown).

Activation of PKC Induces Dephosphorylation at Serine 268 and Phosphorylation at Serine 873. To identify pathways and mechanisms that modulate p120 function, we investigated the effects of direct PKC activation, which increases the permeability of cell monolayers and induces p120 dephosphorylation in several cell types (*22*). To pinpoint the affected site(s), phosphotryptic maps of mp120-1A were generated in HCT116 cells in the presence and absence of phorbol 12,13-dibutyrate (PDBu), a widely used PKC activator. The level of phosphorylation of S268 (spot 3) was substantially decreased by PDBu treatment (Figure 6A, compare panel b to panel a), and pretreatment of cells with bisindolylmaleimide I (BisI), a specific PKC inhibitor, blocked this effect (Figure 6A, panel c). Total levels of p120 phosphorylation were reduced by 40% after PDBu treatment (data not shown), suggesting partial dephosphorylation at other sites. These data suggest that PKC activation indirectly regulates p120 by inactivation of p120 S/T kinases or activation of p120 S/T phosphatases.

Surprisingly, PKC activation strongly induced phosphorylation of a novel series of tightly clustered peptides, which were collectively termed spot 10 (Figure 6A, panel b). This effect was also blocked by pretreatment of cells with BisI (Figure 6A, panel c), indicating a direct requirement for PKC activation. This result was unexpected because all previous reports of PKC-induced effects reflect p120 dephosphorylation, as evidenced by direct measurements of total S/T phosphorylation changes, and by the nature of the p120 bandshift on SDS−polyacrylamide gels. The mobility of spot 10 suggested hydrophilic peptide(s) with high ratios of charge to molecular weight, and PAA showed that the phosphorylated residue for this spot was serine (Figure 6B, panel a). Several candidates were tested, and mutation of S873 to alanine eliminated the entire cluster (Figure 6B, compare panel c to panel b), indicating that all of these spots were derived from peptides containing S873. Figure 6C shows the location of this novel site just amino-terminal to the beginning of the alternatively spliced sequence termed exon A. The sequence flanking S873 reveals a PKC consensus sequence (S-X-K/R), but only if exon A is present. The multiple spots associated with tryptic digestion of this peptide are due to the fact that trypsin does not cleave the

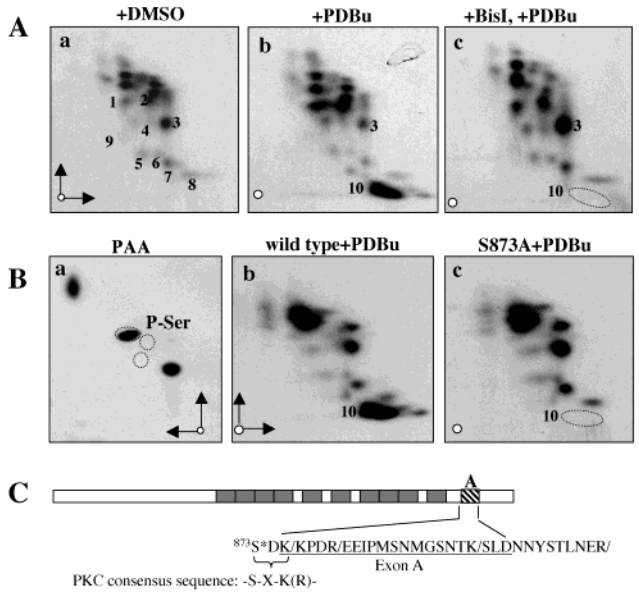

FIGURE 6: Activation of PKC decreases the level of phosphorylation of S268 and induces phosphorylation of S873. (A) HCT116 cells were transiently transfected with mp120-1A and [^{32}P]orthophosphate labeled *in vivo*. Cells were treated with vehicles (DMSO) (panel a) or 200 nM PDBu (panels b and c) for 30 min. In panel c, 2.5 μM BisI was added to the medium 5 min before PDBu was added. The transfected p120 was recovered and subjected to phosphotryptic mapping. PDBu treatment decreased the extent of phosphorylation at S268 (spot 3) and strongly induced phosphorylation of a new group of peptides (spot 10). Both effects are blocked by prior treatment with BisI, a potent PKC inhibitor. (B) Identification of S873 as the phosphorylation site for spot 10. (a) Phosphoamino acid analysis of spot 10 showing exclusive labeling on serine. (b and c) HCT116 cells were transiently transfected with wild-type mp120-1A or the same construct containing an S873A mutation. Cells were labeled *in vivo* and treated with 200 nM PDBu for 30 min. Tryptic phosphopeptide maps revealed that the S873A mutation completely eliminated spot 10. (C) Schematic showing the sequence of the S873 peptide(s). Note that S873 is in a PKC consensus sequence only when alternatively expressed exon A is present.

Lys−Pro (K−P) bond and does not cleave efficiently at Lys−Lys (K−K) or Arg−Glu (R−E) junctions. These data suggest that PKC directly phosphorylates p120 at S873.

Analysis of p120 S/T Phosphorylation and Staurosporine Effects in Colo205 Cells. Colo205 cells are normally poorly adhesive. Treatment with staurosporine, a broad spectrum protein kinase inhibitor, dramatically restores adhesion and induces a p120 bandshift indicative of S/T dephosphorylation (*16*) (see also Figure 7A). Thus, it has been proposed that the adhesive defects in Colo205 cells are caused by alterations in p120 phosphorylation (*16*). To test this hypothesis, we identified the staurosporine sensitive site(s) and attempted to mimic the effects of staurosporine by expressing the relevant mutants. Tryptic maps of both ectopic (stably transfected murine p120) and the endogenous (human) p120 were generated from Colo205 cells with or without staurosporine treatment. PDBu was also tested for comparison. Interestingly, the S268 site (spot 3), which was dephosphorylated by PKC activation (Figure 7C), was even more potently dephosphorylated in response to staurosporine (Figure 7B, compare panel b to a, or panel d to c). In contrast, S873 (spot 10) was unaffected, despite the fact that it is strongly induced by PKC activation, which suggests that staurosporine acts on kinase(s) or phosphatase(s) downstream of PKC. The effects of PDBu and staurosporine on p120 S/T phosphorylation are summarized in Figure 7D.

Interestingly, the T910 spot (spot 8) was absent from maps of endogenous p120 in Colo205 cells (Figure 7B, panels a and b), even though T910 was prominently phosphorylated in p120 from other human cell lines. To determine whether the signaling pathway(s) responsible for this event was defective, we introduced wild-type murine p120-3A and generated tryptic maps. The murine p120 was efficiently phosphorylated at T910 (Figure 7B, panels c and d), suggesting that the absence of phosphorylation at this site in the endogenous Colo205 p120 was not due to a deficiency in the relevant signal pathway(s). We also analyzed the endogenous Colo205 p120 by RT-PCR and cDNA sequencing of its C-terminal end to determine whether the Colo205 p120 is mutated at this site. However, analysis of 12 different cDNA clones revealed only wild-type sequences in the vicinity of T910. Since the amino acid sequences of human and murine p120 are identical in this region, and Colo205 p120 is not mutated, it is not clear why this site is selectively unphosphoryated in Colo205 cells.

A Model Summarizing the Role of PKC in Signaling Pathways that Regulate p120. Our data indicate a role for PKC in regulating p120 (Figure 8). S873 contains a PKC consensus motif and is strongly phosphorylated after PKC activation, suggesting that this site is a direct PKC target. Other sites are indirectly affected, as illustrated in the model. Serine 268 is most prominently affected, and its dephosphorylation occurs downstream of multiple signaling pathways that activate PKC. The data directly connect signaling through PKC with specific sites of p120 phosphorylation.

DISCUSSION

Accumulating evidence suggests that S/T phosphorylation of p120 may directly regulate p120 and E-cadherin function (*16*, *17*, *22*, *23*), and PKC has been widely implicated as an important signaling intermediate (*22*). Identifying the specific contributions of p120 modifications, however, is currently not possible because the signaling pathways acting on p120 simultaneously act on other substrates and pathways as well. Moreover, as is the case for p120 tyrosine phosphorylation (*21*), p120 is phosphorylated at multiple S/T sites, each of which may have crucial but separate consequences (*36*). Therefore, to discriminate p120-specific and phosphorylation site-specific functions from other consequences of signaling, it is necessary to first directly identify the relevant sites, as well as the kinases that phosphorylate them. As an important step toward these goals, we have mapped the major p120 S/T phosphorylation sites, and directly identified sites associated with PKC activation.

Table 1 shows the location of the newly identified S/T sites as well as the tyrosine phosphorylation sites (*21*) identified previously. Most of these sites are tightly clustered in a region comprising approximately 100 amino acids located just amino-terminal to the Arm domain. This region has been termed the phosphorylation domain because most of the previously identified tyrosine phosphorylation sites are located there (*21*). Thus, the majority of tyrosine, serine, and threonine phosphorylation sites are restricted to a 100-amino acid stretch implicated previously in the regulation of p120 function. On the other hand, S873 (spot 10) and

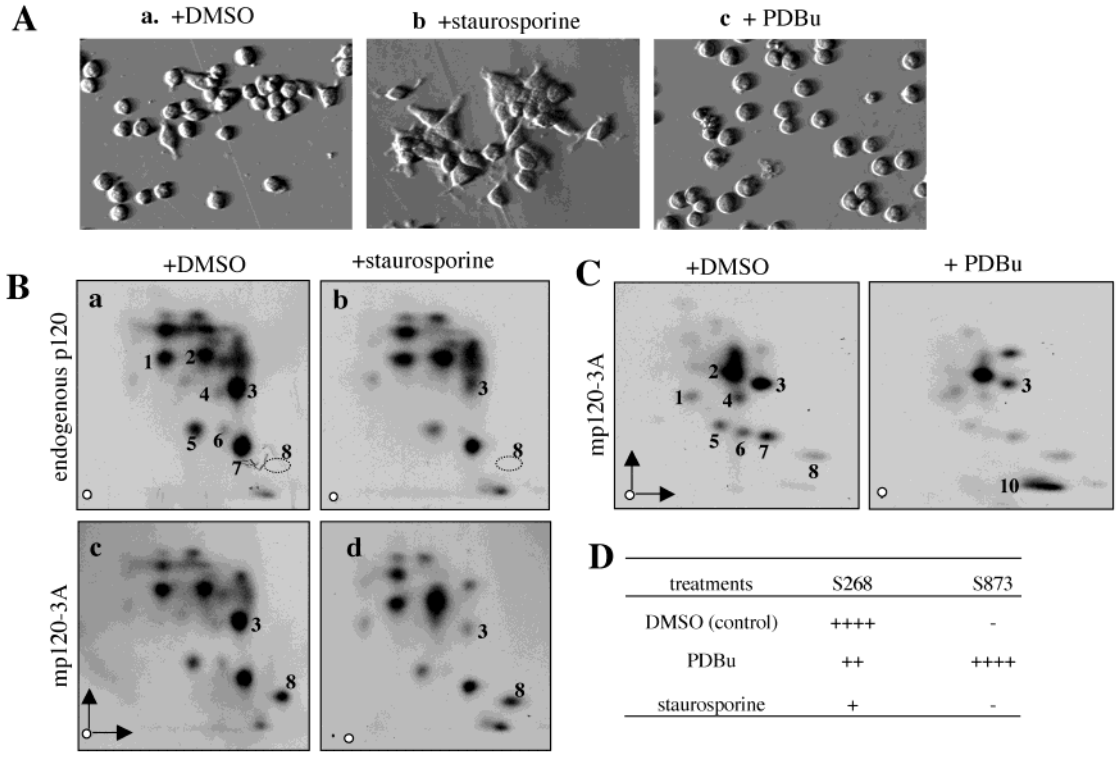

FIGURE 7: Staurosporine induces potent dephosphorylation at S268 in Colo205 cells. (A) Colo205 cells were treated with vehicle alone (DMSO) (panel a), staurosporine (100 nM) (panel b), or PDBu (200 nM) (panel c) for 6 h. Staurosporine, but not PDBu treatment, induces morphology and adhesive changes in Colo205 cells. (B) Staurosporine treatment causes significant p120 dephosphorylation at S268. Parental Colo205 cells (panels a and b) or a stable Colo205 cell line expressing ectopic mp120-3A (panels c and d) was metabolically labeled with [^{32}P]orthophosphate and treated for 6 h with vehicle alone (DMSO) or staurosporine (100 nM), as indicated. Endogenous p120 (panels a and b) or ectopic murine p120 (panels c and d) was immunoprecipitated and subjected to phosphotryptic mapping. Note that T910 (spot 8) is absent in endogenous p120 from Colo205 cells (panels a and b), but present in ectopic murine p120 overexpressed in the same cells (panels c and d). (C) Effects of PDBu on p120 phosphorylation in Colo205 cells. Two-dimensional tryptic maps of mp120-3A were generated from cells stably expressing mp120-3A treated with vehicle alone (DMSO) or PDBu (200 nM) for 30 min. The new spot (over spot 3) that showed up after PDBu treatment in this experiment has not been identified. (D) Summary of the effects of PDBu and staurosporine treatments on p120 phosphorylation at S268 and S873.

T910 (spot 8) are located in the carboxy-terminal end, revealing a new regulatory region. So far, the Arm domain itself does not seem to contain prominent phosphorylation sites, although the site associated with spot 2 has not yet been located, and we cannot rule out important roles for minor phosphorylation sites that were not identified.

Both PKC activators, and staurosporine (a relatively nonspecific kinase inhibitor), result in significant dephosphorylation at S268. Since S268 is dephosphorylated in response to PKC activation, the action of PKC on S268 is clearly indirect. Thus, PKC activity leads to inactivation of S268 kinase(s) or activation of S268 phosphatase(s). The effects of staurosporine on this site were particularly pronounced, suggesting that staurosporine directly inhibits the S268 kinase. These results focus attention on S268 phosphorylation as a potential modulator of p120 and cadherin function. In addition, PKC activators strongly induced phosphorylation at S873. Sequence analysis of S873 reveals a PKC consensus sequence, suggesting that S873 may be directly targeted by members of the PKC family. This result was surprising because all previous data associated with PKC-activation predicted p120 dephosphorylation. The result highlights the importance of direct mapping studies, as opposed to interpreting band shifts or changes in total phosphorylation. Interestingly, the PKC consensus sequence around S873 exists only when exon A is present. Thus, one role for exon A is to provide the consensus sequence necessary for PKC-induced regulation of p120 via S873 phosphorylation.

Phosphorylation of p120 *in vitro* by GSK3β gave rise to four spots, which comigrated exactly with constitutively phosphorylated peptides 4−7 observed on the *in vivo* maps. All four phosphopeptides were eliminated by mutation of S252 and T310 to alanine, indicating that these two sites account for all of the GSK3β-induced spots. The selectivity of GSK3β for these two sites was striking, and they were constitutively present on all *in vivo* maps. However, the physiologic relevance is unclear because treatment of cells with GSK3β inhibitors did not eliminate the spots from maps generated from *in vivo* samples.

By mutating the mapped S/T sites to alanine, we were able to directly address the hypothesis that S/T p120 phosphorylation changes account for the staurosporine-induced rescue of adhesion in Colo205 cells (*16*). p120 isoform 4A lacks the phosphorylation domain and dramatically rescues the adhesive defect in Colo205 cells (*16*). Other treatments that rescue Colo205 cell adhesion include brief trypsinization and addition of staurosporine, both of which induce a p120 bandshift that is indicative of S/T dephosphorylation. We find, however, that direct mutation of these sites, both individually and together, does not mimic the effects of deleting the amino-terminal end (data not shown). Moreover, PKC activation by PDBu also had little effect on Colo205 adhesion even though both PKC activation and

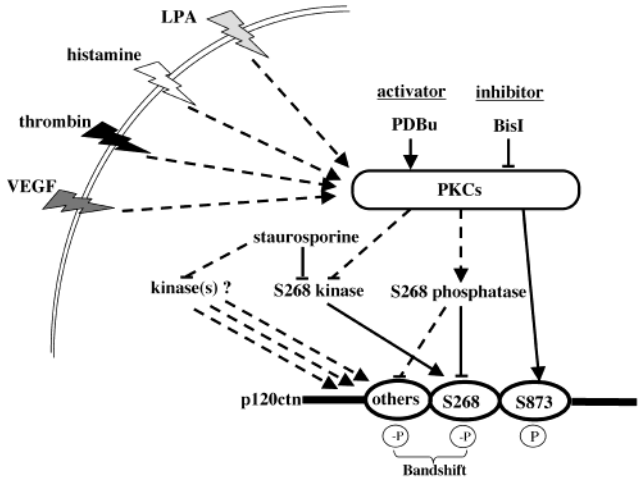

FIGURE 8: Schematic showing pathways relevant to p120 S/T phosphorylation. PKCs are activated by pharmacologic agent PDBu, or in response to extracellular stimulation of physiologically relevant receptors, including those for VEGF, thrombin, histamine, and LPA. Many of these agents have significant effects on cell morphology, adhesion, and motility. Our data strongly suggest that PKC directly phosphorylates p120 at S873. PKC activation also induces dephosphorylation at S268, which is caused indirectly by inactivation of S268 kinase(s) and/or activation of S268 phosphatase(s). Staurosporine also strongly induces dephosphorylation at S268. Thus, staurosporine and PKC may affect a common pathway that brings about dephosphorylation at S268. The data also suggest that PKC stimulation induces partial dephosphorylation at many of the "other sites", along with the more striking dephosphorylation at S268. It appears that these effects are together responsible for the p120 bandshift associated with PKC activation.

staurosporine induce p120 dephosphorylation at S268. Thus, the negative regulatory effects of the p120 amino terminus require its physical presence and cannot be duplicated by mutation of the S/T sites in this region.

The close link between the p120 bandshift and S/T dephosphorylation has been demonstrated previously (*16*, *22*, *23*), but the data given here are the first pieces of information regarding individual sites. Simultaneous mutation of the six major S/T sites resulted in a protein that was always bandshifted, but none of the single S/T to A mutations was sufficient. Extensive dephosphorylation at S268 was invariably correlated with the bandshift, although mutation of this site to alanine did not by itself result in a bandshifted protein. Thus, the approximate 40% decrease in the overall level of p120 S/T phosphorylation by PKC activation may also play a role. Because the direction of the bandshift is indicative of dephosphorylation, the induced phosphorylation at S873 was surprising. Nonetheless, this was the most striking consequence of PKC activation, and strongly implicates this site in direct modulation of p120 activity by PKC.

Whereas β-catenin is tightly associated with cadherins, p120 is thought to associate loosely, and some cells appear to have a significant pool of p120 which is not associated with cadherin (*14*, *37*). We and others have shown previously that cadherin-associated p120 is strongly phosphorylated and that unbound (cytoplasmic) p120 pools are not phosphorylated. Interestingly, alanine mutation of the individual S/T sites, or simultaneous alanine mutation of the six major S/T sites, had no effect on p120 binding to E-cadherin in co-immunoprecipitation assays (data not shown). Thus, S/T phosphorylation of p120 does not directly regulate its E-cadherin binding role, which is mediated by the Arm domain.

A working model showing pathways related to p120 S/T phosphorylation is illustrated and described in Figure 8. Several of the pathways postulated to regulate p120 (and adhesion) through PKC are shown. Our data clearly link PKC activation to p120 phosphorylation at S873, and suggest that PKC directly phosphorylates this site. Indirect regulation of S268 phosphorylation (and several other sites) requires other kinases and phosphatases downstream of PKC. Because many of the acute changes in adheren junction structure and function induced by agents such as thrombin, LPA, and histamine involve PKC activation, it is likely that these p120 phosphorylation sites have important roles in adhesion. It is now possible to directly study these events and isolate the p120-dependent consequences.

REFERENCES

1. Reynolds, A. B., Roesel, D. J., Kanner, S. B., and Parsons, J. T. (1989) *Mol. Cell. Biol. 9*, 629−638.
2. Reynolds, A. B., Herbert, L., Cleveland, J. L., Berg, S. T., and Gaut, J. R. (1992) *Oncogene 7*, 2439−2445.
3. Reynolds, A. B., Daniel, J., McCrea, P. D., Wheelock, M. J., Wu, J., and Zhang, Z. (1994) *Mol. Cell. Biol. 14*, 8333−8342.
4. Shibamoto, S., Hayakawa, M., Takeuchi, K., Hori, T., Miyazawa, K., Kitamura, N., Johnson, K. R., Wheelock, M. J., Matsuyoshi, N., Takeichi, M., et al. (1995) *J. Cell Biol. 128*, 949−957.
5. Staddon, J. M., Smales, C., Schulze, C., Esch, F. S., and Rubin, L. L. (1995) *J. Cell Biol. 130*, 369−381.
6. Takeichi, M. (1991) *Science 251*, 1451−1455.
7. Herrenknecht, K., Ozawa, M., Eckerskorn, C., Lottspeich, F., Lenter, M., and Kemler, R. (1991) *Proc. Natl. Acad. Sci. U.S.A. 88*, 9156−9160.
8. Nagafuchi, A., Takeichi, M., and Tsukita, S. (1991) *Cell 65*, 849−857.
9. Knudsen, K. A., Soler, A. P., Johnson, K. R., and Wheelock, M. J. (1995) *J. Cell Biol. 130*, 67−77.
10. Nieset, J. E., Redfield, A. R., Jin, F., Knudsen, K. A., Johnson, K. R., and Wheelock, M. J. (1997) *J. Cell Sci. 110* (Part 8), 1013−1022.
11. Anastasiadis, P. Z., Moon, S. Y., Thoreson, M. A., Mariner, D. J., Crawford, H. C., Zheng, Y., and Reynolds, A. B. (2000) *Nat. Cell Biol. 2*, 637−644.
12. Anastasiadis, P. Z., and Reynolds, A. B. (2001) *Curr. Opin. Cell Biol. 13*, 604−610.
13. Noren, N. K., Liu, B. P., Burridge, K., and Kreft, B. (2000) *J. Cell Biol. 150*, 567−580.
14. Grosheva, I., Shtutman, M., Elbaum, M., and Bershadsky, A. D. (2001) *J. Cell Sci. 114*, 695−707.
15. Magie, C. R., Pinto-Santini, D., and Parkhurst, S. M. (2002) *Development 129*, 3771−3782.
16. Aono, S., Nakagawa, S., Reynolds, A. B., and Takeichi, M. (1999) *J. Cell Biol. 145*, 551−562.
17. Ohkubo, T., and Ozawa, M. (1999) *J. Biol. Chem. 274*, 21409−21415.
18. Thoreson, M. A., Anastasiadis, P. Z., Daniel, J. M., Ireton, R. C., Wheelock, M. J., Johnson, K. R., Hummingbird, D. K., and Reynolds, A. B. (2000) *J. Cell Biol. 148*, 189−202.
19. Anastasiadis, P. Z., and Reynolds, A. B. (2000) *J. Cell Sci. 113*, 1319−1334.
20. Ireton, R. C., Davis, M. A., van Hengel, J., Mariner, D. J., Barnes, K., Thoreson, M. A., Anastasiadis, P. Z., Matrisian, L., Bundy, L. M., Sealy, L., Gilbert, B., van Roy, F., and Reynolds, A. B. (2002) *J. Cell Biol. 159*, 465−476.
21. Mariner, D. J., Anastasiadis, P., Keilhack, H., Bohmer, F. D., Wang, J., and Reynolds, A. B. (2001) *J. Biol. Chem. 276*, 28006−28013.
22. Ratcliffe, M. J., Rubin, L. L., and Staddon, J. M. (1997) *J. Biol. Chem. 272*, 31894−31901.
23. Ratcliffe, M. J., Smales, C., and Staddon, J. M. (1999) *Biochem. J. 338*, 471−478.
24. Kanner, S. B., Reynolds, A. B., and Parsons, J. T. (1991) *Mol. Cell. Biol. 11*, 713−720.
25. Wong, E. Y., Morgan, L., Smales, C., Lang, P., Gubby, S. E., and Staddon, J. M. (2000) *Biochem. J. 346* (Part 1), 209−216.
26. Lynch, J. J., Ferro, T. J., Blumenstock, F. A., Brockenauer, A. M., and Malik, A. B. (1990) *J. Clin. Invest. 85*, 1991−1998.

27. Lum, H., and Malik, A. B. (1994) *Am. J. Physiol. 267*, L223−L241.
28. Sandoval, R., Malik, A. B., Minshall, R. D., Kouklis, P., Ellis, C. A., and Tiruppathi, C. (2001) *J. Physiol. 533*, 433−445.
29. Wu, J., Mariner, D. J., Thoreson, M. A., and Reynolds, A. B. (1998) *Hybridoma 17*, 175−183.
30. Daniel, J. M., and Reynolds, A. B. (1995) *Mol. Cell. Biol. 15*, 4819−4824.
31. Van der Geer, P. (1994) *Cell Biology: A laboratory handbook*, pp 422−448, Academic Press, London.
32. Downing, J. R., and Reynolds, A. B. (1991) *Oncogene 6*, 607−613.
33. Salic, A., Lee, E., Mayer, L., and Kirschner, M. W. (2000) *Mol. Cell 5*, 523−532.
34. Polakis, P. (2000) *Genes Dev. 14*, 1837−1851.
35. Polakis, P. (2001) *Cell 105*, 563−566.
36. Cohen, P. (2000) *Trends Biochem. Sci. 25*, 596−601.
37. Papkoff, J. (1997) *J. Biol. Chem. 272*, 4536−4543.

BI034597H